

Ringling phenomenon in silica microspheres

Chunhua Dong (董春华), Changling Zou (邹长铃), Jinming Cui (崔金明), Yong Yang (杨勇),
Zhengfu Han (韩正甫)*, and Guangcan Guo (郭光灿)

Key Lab of Quantum Information, University of Science and Technology of China, Hefei 230026

*E-mail: zfhan@ustc.edu.cn

Received December 12, 2008

Whispering gallery modes in silica microspheres are excited by a tunable continuous-wave laser through the fiber taper. Ringing phenomenon can be observed with high frequency sweeping speed. The thermal nonlinearity in the microsphere can enhance this phenomenon. Our measurement results agree very well with the theoretical predictions by the dynamic equation.

OCIS codes: 140.3410, 140.4780, 140.6810.

doi: 10.3788/COL20090704.0299.

Whispering gallery modes (WGMs) in microresonators are of current interest because of their high quality factor (Q) values and small mode volumes at optical frequencies^[1,2]. Microresonators possessing WGMs are considered to be the most promising candidates for a large variety of optical applications, such as ultra-low-threshold lasing^[3], sensing^[4,5], radiation-pressure-induced amplification or cooling of mechanical oscillations^[6–8], cavity quantum electro dynamics (QED)^[9–11], and for their potential in future applications, e.g., quantum information processing^[12]. It is well known that the spectra can be obtained by using a scanning technique in which the excitation wavelength of incident light is swept through the resonances of the microcavity^[13]. The transmission spectrum is found to be inflected by sweeping speed^[14] or input power^[15]. In addition, a fast sweeping of the cavity resonant wavelength induces a ringing phenomenon which was observed in the fiber ring resonator^[16,17].

In this letter, we report the experimental observation of a ringing phenomenon in the silica microspheres excited by a tunable continuous-wave (CW) laser and formulate the dynamical behavior for microsphere systems. The WGM resonator is usually excited by an external coupler, such as tapered fiber, which we have used in our study. When the probe light sweeps through the resonant WGM, the input power will be coupled into the microsphere. Subsequently, the damped photons leaked into the taper whose phase was modulated by the cavity, causing it to interfere with the probing light. This interference eventually appeared as a ringing phenomenon in the transmission of the high- Q WGMs. A Q value of 10^8 corresponding to cavity damping time of 50 ns has been readily achieved in non-doped spheres^[18]. Therefore, a high- Q microsphere resonator such as the one used here would allow this ringing phenomenon to be easily visible and with equation of motion, taking into account the thermal influence, we will show that ringing can be amplified by increasing the input power.

For experimental studies of dynamical behavior for the microsphere system, we used a tunable, single frequency, narrow linewidth (< 300 kHz) external-cavity laser in the 780-nm band. The laser light was coupled into the microsphere through a fiber taper ($\sim 1 \mu\text{m}$) which also helps

coupling light out of the microsphere. The output light was detected by a 125-MHz low-noise photo-receiver, which was connected to a digital oscilloscope to measure the transmission spectra. The microsphere used in our experiment was fabricated by melting the tapered tip of a fiber using a CW CO_2 laser. The coupling strength between the tapered fiber and the microsphere could be adjusted by changing the air gap between them, which was controlled by a high resolution translation stage, with a step resolution in order of 20 nm.

Figure 1(a) shows a typical transmission spectrum, where the transmission dips correspond to the WGM resonances in the silica microsphere with a diameter of $39 \mu\text{m}$. The measured free spectral range (FSR) describing the distance between two adjacent angular modes is about 3.4 nm, which is in good agreement

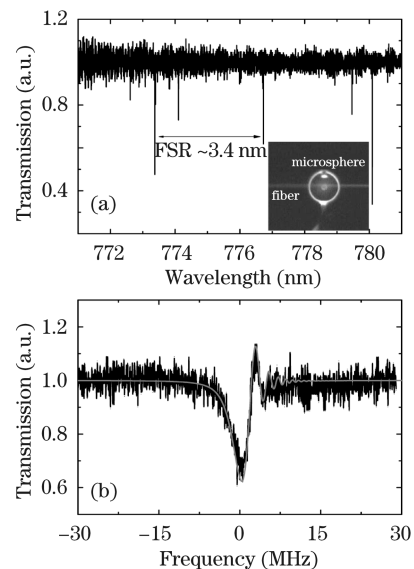


Fig. 1. (a) Typical transmission spectrum of a silica microsphere with a diameter of $39 \mu\text{m}$. The transmission dips correspond to the WGM resonances. Inset: the optical image of microsphere coupling with a low-loss fiber taper. (b) Enlarged mode spectrum at 780 nm measured at sweeping speed $d\nu(t)/dt = 12.5 \text{ MHz}/\mu\text{s}$ and input power $\sim 2 \mu\text{W}$. The smooth line represents the theoretical calculation with $Q_0 = 2.3 \times 10^8$ and $Q_{\text{ex}} = 14.3 \times 10^8$.

with theoretically calculated FSR $\sim \lambda^2/(n_0\pi D)$, where $n_0 = 1.46$ is the refractive index of silica and D is the diameter of the microsphere. Figure 1(b) depicts a single WGM at 780 nm which is measured at a scanning frequency speed $d\nu/dt = 12.5$ MHz/ μ s [$\nu = (\omega(t)/2\pi)$] and input power of 2μ W when the thermal line broadening is neglected. Obviously, there exists ringing phenomenon in the tail of the transmission. It is induced by interference. First, photons coupled to cavity through fiber taper can damply leak for a long time, due to the high Q factor of the cavity. Its phase is then modulated by the cavity. When the time scale of sweeping speed is comparable to the lifetime of the photons, the modulated photons leaking from the cavity will interfere with the probing light whose phase is not modulated. This interference will cause an oscillation in the tail of the transmission, which has been discussed by several authors^[16,19,20]. To explain this phenomenon, we use the dynamic equation governing the intracavity field:

$$\frac{dE_C(t)}{dt} = -[\gamma_c + \gamma_{ex} + i\Delta\omega(t)] E_C(t) + i\frac{\eta}{\tau_c} E_{in}(t), \quad (1)$$

where $\gamma_c = (\omega_0/2Q_0)$ and $\gamma_{ex} = (\omega_0/2Q_{ex})$ are the decrement of internal losses and the decrement of coupler device with Q_0 and Q_{ex} being the intrinsic and external quality factors, respectively; $\eta = \sqrt{2\tau_c\gamma_{ex}}$ is the effective coupling coefficient; τ_c is the cavity round-trip time; $E_{in}(t)$ is the input field; $E_C(t)$ is the electronic field amplitude of the WGM; $\Delta\omega(t) = \omega_p(t) - \omega_0$, $\omega_p(t)$ is the frequency of the external field, and ω_0 is the unperturbed resonant frequency. The normalized transmission of the cavity is $T(t) = |1 + i\eta E_C(t)/E_{in}(t)|^2$ and a plot of the theoretical values is shown in the Fig. 1(b). The simulated values coincide well with the experimental data.

Figure 2 represents the resonator transmission against the frequency for different loading conditions and different sweeping speeds. For high- Q WGMs or higher

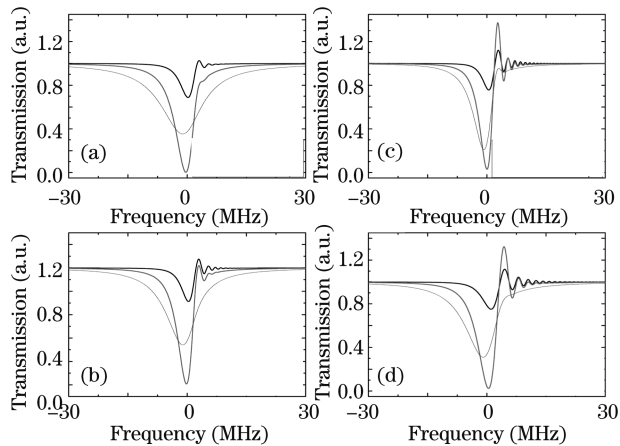


Fig. 2. Calculated transmission for different coupling regimes with different Q_0 and different $d\nu/dt$. Solid lines, $Q_{ex} = 10Q_0$; dashed lines, $Q_{ex} = Q_0$; dotted lines, $Q_{ex} = 0.25Q_0$. For the theoretical calculation, the quality factor Q_0 and sweeping speed $d\nu/dt$ are used with (a) 1.5×10^8 , 12.5 MHz/ μ s; (b) 2×10^8 , 12.5 MHz/ μ s; (c) 3×10^8 , 12.5 MHz/ μ s; (d) 2×10^8 , 25 MHz/ μ s.

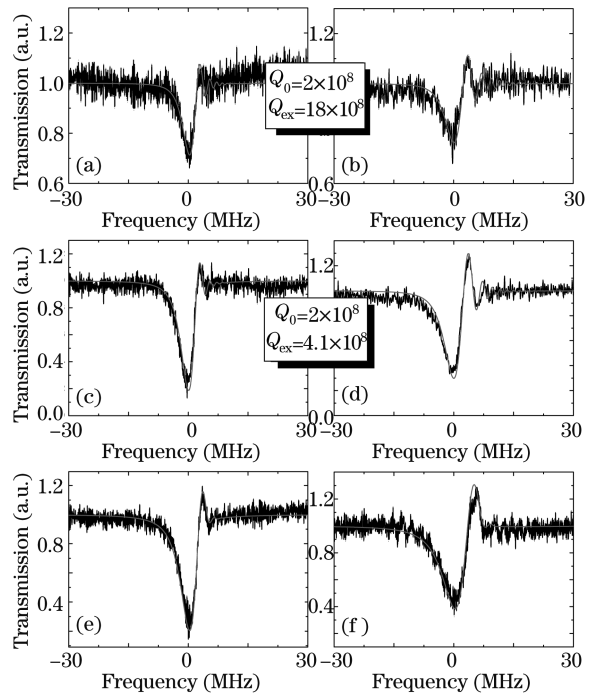


Fig. 3. Slow and fast scanning experimental results and theoretical calculation (smooth lines) for different coupling regimes. For the theoretical calculations, Q_0 and Q_{ex} are used with (a), (b) 2×10^8 , 18×10^8 ; (c), (d) 2×10^8 , 4.1×10^8 ; (e) 4×10^8 , 1.1×10^8 ; and (f) 5×10^8 , 0.7×10^8 , respectively. The left column corresponds to the sweeping speed $d\nu/dt = 12.5$ MHz/ μ s, while the right column corresponds to 25 MHz/ μ s. The excitation power used is 2μ W when the thermal effect is negligible.

frequency sweeping speed, we obtain the ringing phenomenon. The ringing phenomenon is caused by the difference in time for different light components in the cavity resonator to reach a point of destructive interference. To confirm the theoretical analysis, Fig. 3 shows the experimental results (black lines) and theoretical calculation (red lines) for different loading conditions and different sweeping speeds. For the same coupling regime, the ringing phenomenon can be easily produced at fast scanning frequency speed, as shown in Figs. 3(a)–(d). The ringing phenomenon is not obvious at the regime of overcoupling with $Q_0 = 2 \times 10^8$, predicted in Figs. 2(b) and (d), whereas for higher Q_0 , we obtain the ringing phenomenon, as shown in Figs. 3(e) and (f).

When we increase the input power, the cavity medium with a thermal expansion coefficient of ε and a thermo-optic coefficient of dn/dT is considered and the thermal line broadening becomes marked^[15,21,22]. Suppose the cavity resonant frequency, $\omega_0(t)$, can be written as

$$\omega_0(t) = \omega_0 \left[1 - \left(\varepsilon + \frac{1}{n_0} \frac{dn}{dT} \right) \Delta T(t) \right], \quad (2)$$

where $\Delta T(t)$ is the power induced temperature change within the cavity mode volume. For fused silica, we calculated the temperature coefficient of the resonant frequency to be $\varepsilon + (1/n_0)(dn/dT) = 6 \times 10^{-6}$ (1/ $^\circ$ C)^[23]. The induced Kerr nonlinearity is negligible in this case. The thermal-dynamic equation governing the induced

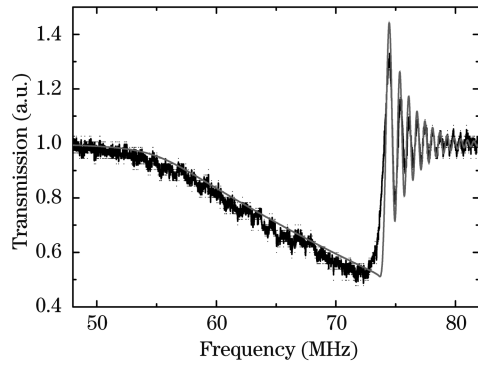


Fig. 4. Dynamical thermal behavior of microsphere: optical transmission as a function of frequency. The experimental data are measured at $d\nu(t)/dt = 12.5$ MHz/ μ s, and the smooth line represents calculated values. The cold resonant wavelength of the microsphere is $\lambda_0 = 778.3$ nm and its quality factors are $Q_0 = 2 \times 10^8$, $Q_{\text{ex}} = 11 \times 10^8$. The input power is 220 μ W.

temperature change^[21,24] is

$$C_p \frac{d\Delta T(t)}{dt} = -K\Delta T(t) + I \frac{1}{\left(\frac{\omega_p(t) - \omega(t)}{\Delta\omega/2}\right)^2 + 1}, \quad (3)$$

where C_p , K , and I are the heat capacity, the thermal conductivity between the cavity mode volume and the surroundings, and the power that actually heats the cavity, respectively; $\Delta\omega(t) = \omega_p(t) - \omega_0(t)$.

Using Eqs. (1) – (3), it is possible to analytically obtain the transmission of the resonator. Figure 4 shows the experimental result and the calculated WGM transmission as a function of frequency when the thermal line is broadened with an input power of 220 μ W. Obviously, the red shift of resonant wavelength with up-scanning input power is clear with thermal line broadening. The ringing phenomenon is obviously intensified at the abrupt detuning^[21] between the cavity mode and the scanning wavelength.

In summary, the ringing phenomenon in silica microsphere is observed and explained by the dynamic equation. The ringing phenomenon can be observed with higher Q_0 factors and faster sweeping speeds. When thermal drift of the resonance is typically more than the resonant width, thermal effects must be taken into account. We have shown theoretically and experimentally that this ringing phenomenon will be amplified as the input power increases. In addition, the intrinsic quality factor Q_0 and external quality factor Q_{ex} can be distinguished for different coupling regimes.

This work was supported by the National Fundamental Research Program of China (No. 2006CB921900),

the National Natural Science Foundation of China (Nos. 60537020 and 60621064), and the Knowledge Innovation Project of the Chinese Academy of Sciences.

References

1. K. J. Vahala, *Optical Microcavities* (World Scientific, Singapore, 2004).
2. R. K. Chang and A. J. Campillo, *Optical Processes in Microcavities* (World Scientific, Singapore, 1996).
3. L. Yang, T. Carmon, B. Min, S. M. Spillane, and K. J. Vahala, *Appl. Phys. Lett.* **86**, 091114 (2005).
4. A. M. Armani, R. P. Kulkarni, S. E. Fraser, R. C. Flagan, and K. J. Vahala, *Science* **317**, 783 (2007).
5. X. Wang, N. Lü, Q. Tan, and G. Jin, *Chin. Opt. Lett.* **6**, 925 (2008).
6. T. Carmon, H. Rokhsari, L. Yang, T. J. Kippenberg, and K. J. Vahala, *Phys. Rev. Lett.* **94**, 223902 (2005).
7. A. Schliesser, P. Del'Haye, N. Nooshi, K. J. Vahala, and T. J. Kippenberg, *Phys. Rev. Lett.* **97**, 243905 (2006).
8. Y.-S. Park and H. Wang, *Opt. Express* **15**, 16471 (2007).
9. Y.-S. Park, A. K. Cook, and H. Wang, *Nano Lett.* **6**, 2075 (2006).
10. B. Dayan, A. S. Parkins, T. Aoki, E. P. Ostby, K. J. Vahala, and H. J. Kimble, *Science* **319**, 1062 (2008).
11. K. Srinivasan and O. Painter, *Nature* **450**, 862 (2007).
12. Y.-F. Xiao, Z.-F. Han, and G.-C. Guo, *Phys. Rev. A* **73**, 052324 (2006).
13. X. Wu, Y. Xiao, Y. Yang, C. Dong, Z. Han, and G. Guo, *Chin. Opt. Lett.* **5**, 668 (2007).
14. C. Schmidt, A. Chipouline, T. Pertsch, A. Tünnermann, O. Egorov, F. Lederer, and L. Deych, *Opt. Express* **16**, 6285 (2008).
15. H. Rokhsari, S. M. Spillane, and K. J. Vahala, *Appl. Phys. Lett.* **85**, 3029 (2004).
16. D. Ying, H. Ma, and Z. Jin, *Appl. Opt.* **46**, 4890 (2007).
17. Y. Dumeige, S. Trebaol, L. Ghişa, T. K. N. Nguyen, H. Tavernier, and P. Féron, *J. Opt. Soc. Am. B* **25**, 2073 (2008).
18. F. Treussart, V. S. Ilchenko, J. F. Roch, P. Domokos, J. Hare, V. Lefèvre, J.-M. Raimond, and S. Haroche, *J. Lumin.* **76&77**, 670 (1998).
19. J. Poirson, F. Bretenaker, M. Vallet, and A. Le Floch, *J. Opt. Soc. Am. B* **14**, 2811 (1997).
20. A. A. Savchenkov, A. B. Matsko, V. S. Ilchenko, and L. Maleki, *Opt. Express* **15**, 6768 (2007).
21. T. Carmon, L. Yang, and K. J. Vahala, *Opt. Express* **12**, 4742 (2004).
22. V. S. Ilchenko and M. L. Gorodetskii, *Laser Phys.* **2**, 1004 (1992).
23. D. N. Nikogosyan, *Properties of Optical and Laser Related Materials: A Handbook* (Wiley, Chichester, 1997).
24. Y.-S. Park and H. Wang, *Opt. Lett.* **32**, 3104 (2007).